MR Imaging of Reynolds Dilatancy in the Bulk of Smooth Granular Flows

Ken Sakaie,[1] Denis Fenistein,[2] Timothy J. Carroll,[3] Martin van Hecke,[2] and Paul Umbanhowar[4]

[1]*The Cleveland Clinc, 9500 Euclid Ave., Mailcode U-15, Cleveland, OH 44195, USA*
[2]*Kamerlingh Onnes Lab, Universiteit Leiden, Postbus 9504, 2300 RA Leiden, The Netherlands*
[3]*Departments of Biomedical Engineering and Radiology, Northwestern University, 676 N. St. Clair, Suite 1400, Chicago, Il 60611, USA*
[4]*Department of Mechanical Engineering, Northwestern University, Evanston, Illinois 60208, USA*

(Dated: February 1, 2008)

Dense granular matter has to expand in order to flow, a phenomenon known as dilatancy. Here we perform, by means of Magnetic Resonance Imaging, direct measurements of the evolution of the local packing density of a slow and smooth granular shear flow generated in a split-bottomed geometry. The dilatancy is found to be surprisingly strong. The dilated zone follow the region of large strain rate and slowly spreads as a function of time. This suggests that the local packing density is governed by the total amount of local strain experienced since the start of the experiment.

PACS numbers: 45.70.-n, 46.65.+g,

Granular media, such as sand, are conglomerates of dissipative, athermal particles that interact through repulsive and frictional contact forces, and that jam into a disordered configuration when no external energy is supplied [1]. When slowly sheared, granulates flow, but to do so, they must overcome geometrical (steric) hindrance. The resulting expansion of the material is referred to as Reynolds dilatancy [2, 3]. Precise studies of dilatancy are hindered by the opaque nature of granular media, and by the complexity of slow grain flows, which in experimental situations never form a simple linear shear profile [4, 5, 6] — measurements of average densities therefore cannot probe dilatancy. Hence, many basic questions are left unanswered. How much do granular material dilate in the flowing zone? Does the dilatancy depend on the local strain rate? How far does the dilated zone extend? Does the packing density evolve over time?

Here we address these issues by imaging the 3D packing density of smooth and slow granular flows by means of Magnetic Resonance Imaging (MRI). The flows are generated in a split-bottomed shear cell, where the grain flow is driven by the rotation of a bottom disc with respect to a cylindrical container (Fig. 1a). In these systems, a wide shear zone emanates from the edge of the disc, making them well suited for studies of smooth and slow granular flows [6, 7, 8, 9, 10, 11, 12, 13, 14]. In earlier studies, the ratio of the filling height H to the radius of the disc R_s was found to govern the qualitative nature of the flow [7, 8, 9, 10, 11, 12]: When H/R_s is less than 0.6, the central core material rests on and rotates as a solid with the disc. The shear zone then reach the free surface, and the three dimensional shape of the region of large shear resembles the cone of a trumpet [8, 9, 10, 11, 12]. When $H/R_s \gtrsim 0.75$, the flowing zone do not reach the surface but forms a "dome" shaped shear zone in the bulk of the material [9, 10, 11, 12]. For intermediate filling depths there is a crossover regime [11].

By imaging the local packing densities in our shear cell as a function of time and for a range of filling heights, we explore the relation between flow field and dilatancy. The simple picture that emerges is that the amount of dilatancy grows with the total amount of local strain experienced and saturates when the local strain becomes of order one. First, we show that the relative change in density in the flowing zone is rather strong and saturates around 10-15 %. Secondly, we find that the dilated zone slowly spread throughout the system as time progresses. This spread is consistent with the idea that the total, local strain experienced since the start of the experiment governs the amount of dilatancy — to show this, we will reconstruct the flow field in the bulk, combining previously found scaling relations [6, 8, 9, 13] with measurements of the velocity at the surface. Finally, and in contrast to small filling heights ($H/R_s < 0.6$) where the locations of the dilated zone and the shear zone coincide, for deep filling heights a relatively long-lived transient causes the dilated zone to deviate from the late-time shear zone.

Experimental setup — By detecting the signal of protons in oil within seeds, MRI has been used to non-invasively probe the dynamics of granular materials [10, 15, 16, 17]. While various techniques, based on either spin-tagging or employing mixtures of grains with distinct oil concentration, have been used to track grain motion, we are not aware of prior research employing MRI to measure packing densities ϕ. Here, food grade poppy seeds sieved to select diameters of one mm were used. Multiple horizontal slices were acquired in an interleaved fashion to reduce signal saturation effects [18]. Slices were 2 mm thick with in-plane resolution of 1.56 mm x 1.56 mm. Individual seeds are thus not resolved, but the MRI signal probes local packing densities. To compensate for the overall gradients in the signal, we compare signal intensity before and after flow has occurred, and report the relative change in density $\Delta\phi \equiv \phi(t)/\phi(0) - 1$. We employ the azimuthal symmetry of the system to av-

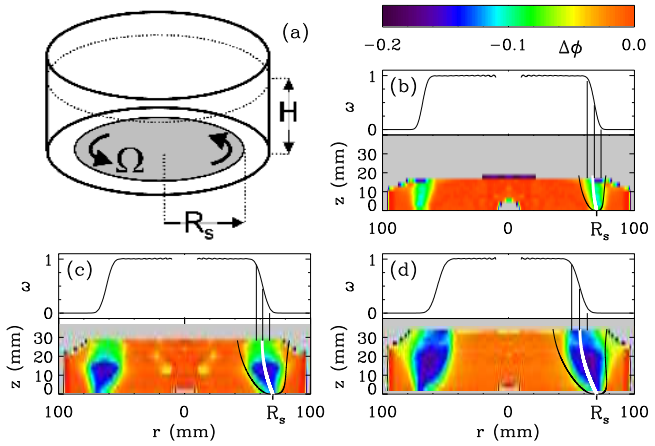

FIG. 1: (Color) (a) Sketch of the split-bottomed shear cell, in which a layer of granular material of depth H is driven by the rotation of a disc of radius R_s with rate Ω. (b-d). Comparison of the surface flow field $\omega(r)$ and the packing density in the bulk after N rotations. (b) $H/R_s = 0.23$ and $N = 2.5$; (c) $H/R_s = 0.41$ and $N = 4$; (d) $H/R_s = 0.51$ and $N = 4$. The straight, vertical lines indicate where $\omega(r)$ reaches 0.1, 0.5 and 0.9, thus indicating the location of the shear zone as observed at the free surface. The white curves are a theoretical prediction for the center of the shear zone based on Eq. 3 [9]. The black curves show examples of the edge of the shear zone, based on Eq. 3 and 4.

erage the data and focus on $\Delta\phi(N, r, z)$, where N, r and z denote the number of rotations of the disc since the start of the experiment and the radial and vertical coordinate respectively.

The experimental geometry placed into the MRI apparatus is a stationary plexiglass drum of inner radius 95 mm in which the bottom disk of radius $R_s = 70$ mm is slowly rotated with a rate Ω of approx $1/8\ s^{-1}$ (see Fig. 1). At this rate, the flow velocities are simply proportional to Ω [6, 7, 8, 9, 10, 11, 12, 13, 14, 17]. The cell is filled with poppy seeds and tapped to obtain a well-compacted initial condition of filling depth H. A layer of seeds is bonded to the side walls and bottom to obtain rough boundaries. To study the temporal evolution of the density, we have obtained images after N rotations of the bottom disc. During the MRI procedure, the disc is stopped — starting and stopping the flow has no appreciable effect on these slow, non-inertial flows. To facilitate direct comparisons to the flow field, we used video imaging to obtain the non-dimensional surface velocity profile $\omega(r)$, defined as the ratio of the time averaged azimuthal velocity to the driving rate Ω [7, 8, 11]. We focus on late times after transients have died out.

Dilated zone and Shear zone for low filling heights — Figure 1 illustrates shear and dilated zones are directly related for low filling heights ($H/R_s \lesssim 0.55$). First, near the surface, the location of the dilated zone and the shear zone coincide. Measurements of the surface velocity profiles $\omega(r)$ are in agreement with earlier studies [7, 8, 10, 11, 13] since we find that

$$\omega(r) = 1/2 + 1/2\ \mathrm{erf}\left[(r - R_c)/W\right] \ , \qquad (1)$$

where the center location R_c in consistent with the simple scaling law:

$$1 - R_c/R_s = (H/R_s)^{5/2} \ . \qquad (2)$$

Figure 1b-d shows that the centers of the dilated and shear zones coincide at the free and bottom surfaces, and that the width of both zones grows similarly with H/R_s.

Second, in the bulk the dilated zone also follow the shear zone. The center of the shear zone throughout the bulk R_c and the vertical coordinate z are related to the geometrical parameters H and R_s by a scaling argument as [9]:

$$z = H - R_c(1 - R_s/R_c(1 - (H/R_s)^{2.5}))^{0.4} \ . \qquad (3)$$

Fig. 1b-d shows that this curve falls into the center of the dilated zone.

Third, data on the width of the shear zone in the bulk, obtained by either excavating colored particles [8, 11] or MRI and numerical studies of the flow field [10, 13], indicate that the shear zone rapidly widen with distance from the bottom disc as [19]

$$W \sim z^{1/3} \ . \qquad (4)$$

We have shown examples of such curves in Fig. 1b-d, and find that they describe the shape of the dilated zone well [19, 20]. Overall, our data clearly suggest that for $H/R_s \lesssim 0.55$ the shear and dilated zones are directly related.

Spread of the dilated zone — Notwithstanding their close relation, the shear zone and dilated zone are not identical. To clarify the relation between dilatancy and flow field further, we show in Fig. 2a the evolution of the density profiles obtained along a number of vertical slices as a function of the number of rotations N.

We first focus on the density profiles for fixed N. The local flow and strain rate vary substantially throughout the shear zone (see below), but in contrast, the dilatancy clearly reaches a plateau value throughout the shear zone. Packing density and local strain rate are thus not directly related. We have found that this maximal dilatancy is similar for all our data sets, and does not vary much with time and depth, except close to the free surface [20]. The amount of dilatancy is substantial, with the densities in the plateau 10-15% lower than the non-sheared regions. To put this number in perspective, disordered packings of spheres span a range in packing densities from 55% (Random Loose Packing) to 64 % (Random Close Packing), with typical densities of poured grains around 60 % [21, 22]. Even though poppy seeds are not perfectly spherical (see Fig. 2b), so that the precise values of these

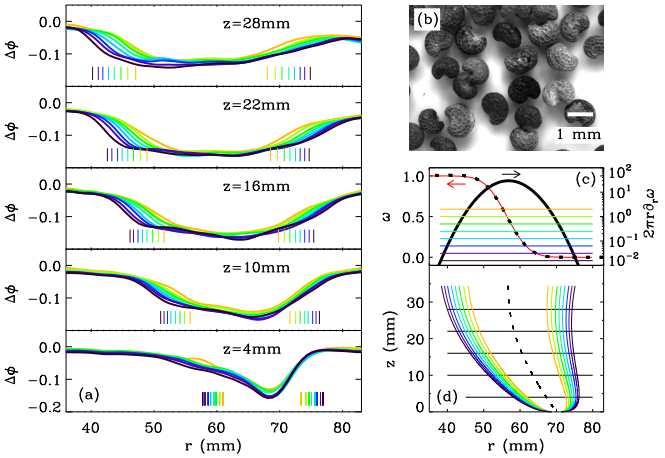

FIG. 2: (Color) (a) Horizontal profiles of the density changes for the data set with $H/R_s = 0.51$ (shown in Fig. 1d), as functions of N and for five values of z as indicated. $N = 1/2, 1, 2, 4, \ldots 64$, with $N = 1/2$ shown in orange, and $N = 64$ in black. The vertical lines indicate estimates of where, after N turns, the local strain rate equals one. (b) Snapshot of the poppy seeds used in this experiment. (c) Surface velocity $\omega(r)$ (dashed), a fit to the error function form of Eq. (1) (red), and the local strain after one rotation $2\pi r\partial_r\omega$ (black, log scale). The horizontal lines indicate where the local strain γ reaches one after N rotations — colors as in panel (a). (d) Illustration of the locations where γ after N rotations reaches one, constructed from the strain at the surface and the scaling laws Eq. (3) (dashed line) and Eq. (4).

numbers may be somewhat different, the observed dilatancy is substantial.

The most striking feature shown in Fig. 2a is that the dilated zone slowly spreads with the number of rotations N [23]. As we will now show, the picture that emerges is that the total amount of strain, not the strain rate, governs the amount of dilatancy — entirely consistent with a quasi-static picture of slow grain flows.

This is illustrated in Fig. 2. Away from the container bottom, vertical gradients are small, and we approximate the total local strain in the bulk after N turns by

$$\gamma = 2\pi N r \partial_r \omega \ . \qquad (5)$$

To obtain $\partial_r\omega$, we start from the surface velocity profile (black dashed curve in Fig. 2c), to which we fit the error function form of Eq. (1) (red curve in Fig. 2c) before taking the derivative to obtain the local strain after one rotation ($2\pi r\partial_r\omega$) (black curve in Fig. 2c, log scale). The horizontal lines in Fig. 2c indicate where the local strain at the surface after N rotations reaches one.

Figure 2d illustrates how we determine the local strain field in the bulk from the surface measurements. We start with the observation that the functional form of $\omega(r)$ in the bulk is also an error function [10, 11]. The center location of this shear zone is given by Eq. 3 (dashed curve in Fig. 2d). Finally, in the bulk the width of the shear zone scales as $z^{1/3}$ [8, 10, 11, 13], so using the measured width of the shear zone at the free surface we can calculate the complete strain rate field. From this we can then deduce, for any number of turns N, where in the bulk the local strain reaches one (colored curves in Fig. 2d).

In Fig. 2a, the density profiles for $N = 1/2, 1, 2, 4, \ldots, 64$ are compared to the location in the bulk where after N turns $\gamma = 1$. We see that, at least qualitatively, the location where the strain reaches one coincides with the edge of the dilated zone. Near the container bottom, the coincidence is less good, but there vertical gradients, deviations from Eq. 4 and boundary effects may be substantial. Nevertheless, our data provides clear evidence that the spreading of the dilated zone is simply caused by the spreading of the position where the local strain becomes of order one with time. This suggests that there is no steady state and that the dilated zone continually expands since the strain rate is nowhere strictly zero [23].

In prior work focussing on the velocity field for similar filling heights, no long time evolution was observed [7, 8, 10, 11, 13]. This does not necessarily disagree with the slow dilatancy. To measure velocities accurately, one requires grains to move substantially in order to average out fluctuations. However, the system is already fully dilated after a local strain of order 1, so that transients in the flow field caused by changes in the density escape detection — essentially, dilatancy happens in the far tails of the velocity profiles [14].

Dilated zone for large filling heights — In Fig. 3a we show the surface velocities and density evolution for $H/R_s = 0.77$. For such deep filling depths, the shear zone emanating from the edge of the disk meet in the middle of the cell and form a dome-like structure, and the surface remains essentially stationary [9, 10, 11, 12]. Simple scaling laws for the flow field like Eqs. (1-4) are not known, but the qualitative features of the dilated zone at early times also show the dome-like shape [9, 10, 11, 12]. For later times the dilated zone spreads throughout large parts of the system, leading to an appreciable elevation and corrugation of the free surface. Slow convection, occurring for large filling heights, leads to the slow growth of a dip in the center of the free surface [10, 11, 24].

In Fig. 3b we show the surface velocities and density evolution for $H/R_s = 0.61$. This corresponds to the intermediate regime, where the velocity profile is weakly asymmetric [11], but there is no precession. We recover this asymmetry of $\omega(r)$, and also note that the center of the surface remains stationary during a short transient. The bulk density evolution reveals that the 3D flow profile is a complex mix between the "trumpet" shape observed for small filling heights and the "dome" shape observed for large filling heights [10, 11, 24]. For early times, all the dilatancy is concentrated in a dome like structure, consistent with the steady surface for early

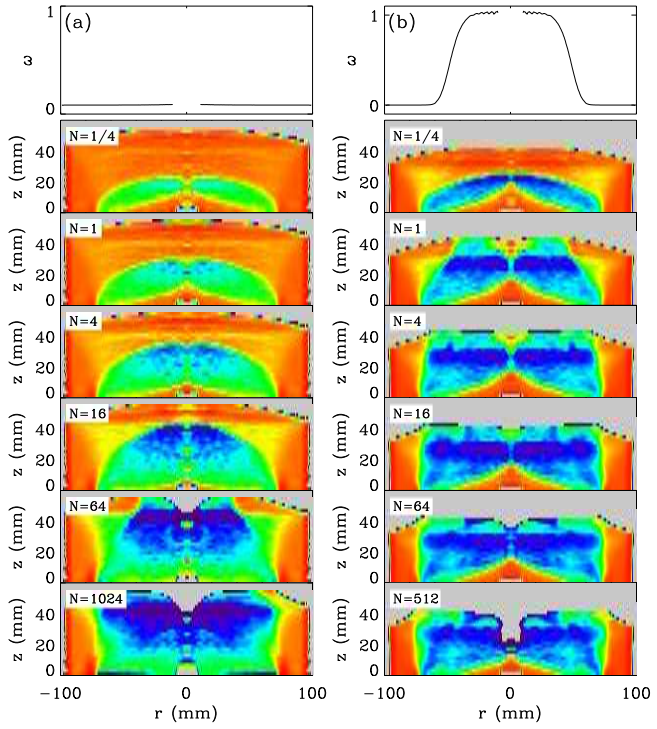

FIG. 3: (Color) Surface velocity profiles and dilatancy maps for (a) $H/R_s = 0.77$ and (b) $H/R_s = 0.61$. See text.

times. For late times, the shear zone evolves to the trumpet shape leading to $\omega \approx 1$ near the center of the surface. We suggest that the symmetry breaking of the surface flow profiles and the dome-like dilated zone might be related [11]. Also here a dip develops near the free surface (the almost vertical shape of this dip for $N = 512$ is an imaging artefact).

Discussion — Our data uncovers how granular media dilate under steady shear [25]: the amount of dilatancy grows with the accumulated strain, and saturates when this strain becomes of order one. This fully dilated state might very well coincide with what in the engineering literature is known as the "critical state", referring to a final state of grain flow where rheological properties stay constant [14]. How general this correspondence is remains to be seen, in particular for shear bands near a boundary or free surface [4, 17].

DF acknowledges support from FOM, and MvH acknowledges support from NWO/VIDI and discussions with X. Cheng.

[1] A. J. Liu and S. Nagel, Nature **396**, 21 (1998).
[2] P. Reynolds, Proc. R. Inst. **2**, 354 (1886); (see Dunstan *et al.*, Nature 336, 52 (1998)).
[3] Note that very loosely packed materials may actually compact upon shearing.
[4] GDR MiDi, Eur. Phys. J. E. **14**, 341 (2004), and references therein; L. Silbert *et al.*, Phys. Rev. E **64**, 051302 (2001).
[5] N. W. Mueggenburg, Phys. Rev. E **71**, 031301 (2005).
[6] M. Depken, M. van Hecke and W. van Saarloos, Phys. Rev. E **73**, 031302 (2006).
[7] D. Fenistein and M. van Hecke, Nature **425**, 256 (2003).
[8] D. Fenistein, J.-W. van de Meent and M. van Hecke, Phys. Rev. Lett. **92**, 094301 (2004).
[9] T. Unger, J. Török, J. Kertész and D. E. Wolf, Phys. Rev. Lett. **92**, 214301 (2004).
[10] X. Cheng *et al.*, Phys. Rev. Lett. **96**, 038001 (2006).
[11] D. Fenistein, J.-W. van de Meent and M. van Hecke, Phys. Rev. Lett. **96**, 118001 (2006).
[12] J. Trk, T. Unger, J. Kertsz, and D. E. Wolf Phys. Rev. E **75**, 011305 (2007).
[13] M. Depken, J. B. Lechman, M. van Hecke, W. van Saarloos and G. S. Grest, accepted for EPL (2007).
[14] A. Ries, D. E. Wolf and T. Unger, arXiv:0704.2392 (2007).
[15] M. Nakagawa, S.A. Altobelli, A. Caprihan, E. Fukushima, E.-K. Jeong, Exp. Fluids **16**, 54 (1993).
[16] E.E. Ehrics *et al.*, Science **267**, 1632 (1995).
[17] D. M. Mueth *et al.*, Nature **406**, 385 (2000).
[18] All measurements were performed on a Siemens Trio 3 Tesla system with a standard 8-channel head coil. Spin-echo acquisitions were used to minimize loss of signal due to field inhomogeneity inherent to a composite material. Given spin-lattice and transverse relaxation times of approximately 300 milliseconds and 20 milliseconds, respectively, the acquisition parameters (repetition time of 1000-1800 milliseconds, echo time of 15 milliseconds, and flip angle of 90 degrees) leave the signal subject to saturation and decay. However, comparison of signal of seeds before and after rotation accounts for systematic errors in signal weighting due to the acquisition parameters. Furthermore, measurements of spin-lattice and transverse relaxation times before and after rotation show no measurable changes, confirming that the signal intensity reflects the density of the seeds.
[19] In [14], the authors find a somewhat different scaling law for the width of the shear zone. With the present MRI resolution, results based on this scaling are not significantly better than those based on Eq. 4.
[20] Surprisingly, near the free surface the dilated zone appears to shrink in width, in qualitative contrast to what has been observed for the shear zone. This appears to be a general feature of the density maps we obtained, and while we cannot exclude imaging artifacts near the free surface, we believe that this is caused by a difference in the initial packing density near the surface — presumable, deep inside the layer where the grains sustain a larger weight, the material is slightly more compacted than near the surface, so that the latter show a smaller relative change in density.
[21] G. Y. Onoda and E. G. Liniger, Phys. Rev. Lett. **64**, 2727 (1990).
[22] D. A. Weitz, Science **303**, 968 (2004).
[23] We have found evidence for continued dilated zone spreading after hundreds of rotations of the bottom disc.
[24] X. Cheng, Private Communications.
[25] For oscillatory shear, the situation is richer, with recompaction and dilatancy competing, see M. Toiya, J. Stambaugh, and W. Losert, Phys. Rev. Lett. **93**, 088001 (2004).